The effect of high speed rail embankments on vibration levels in the near and far field

<**D. Connolly**>, <University of Edinburgh> ***Name of speaker in bold***
<M.C. Forde>, <University of Edinburgh>
<A. Giannopoulos>, <University of Edinburgh>
<P.K. Woodward>, <Heriot Watt University>

Abstract— **The effect of embankment construction materials on the propagation of vibration from railway lines is investigated. The study is undertaken using a newly developed three dimensional numerical model.**

The model is a fully coupled, time domain, finite element model that uses absorbing boundaries to absorb outgoing waves. A multi-body dynamics approach is utilised to provide an excitation mechanism that closely resembles the physical movement of a high speed locomotive. Its prediction capabilities are validated using data collected during field trails conducted on a high speed line between Brussels-Paris.

The model is then used to analyse the effect of embankment conditions on the transmission and propagation of vibrations in both the near and far fields. It is concluded that unless an embankment is constructed using a stiffer material than the natural supporting ground, waveguide effects are prevalent. This causes a trapping of vibration energy within the track structure resulting in elevated vibration levels both within the track and in the surrounding environment.

***Keywords*—Embankment, High speed rail, Railway, Vibration.**

I. INTRODUCTION

The heavier axle loads and higher speeds associated with high speed rail transportation give rise to elevated levels of ground vibration in comparison to traditional rail transport.

To accurately determine the costs associated with vibration mitigation on a new high speed line it is important to be able to predict vibration levels before construction. Early research in this area was undertaken by [1] and [2] and expanded upon by [3]. These approaches focused on closed-form analytical solutions for the purposes of reducing computational requirements.

More recently with advancements in processor technology, the balance of computational railway vibration research has shifted from analytical modelling to numerical approaches such as FEM/BEM (Finite element method / boundary element method). For example, [4] and [5] utilised fully three dimensional FEM approaches to obtain high accuracy estimates of vibration levels. A challenge with such approaches is the reflection of spurious waves from the truncated boundaries and the significant computational demand.

To overcome boundary reflections [6] used a combined FEM/BEM approach where the complex track geometries are modelled using FEM and the unbounded soil domain is modelled using BEM, thus eliminating the requirement for an absorbing boundary.

Despite these advancements in vibration modelling, few researchers have investigated the effect of embankment structures on the propagation of vibration from high speed lines. One of these few investigations was undertaken by [7] who used an analytical approach to approximate an embankment as a cuboidal mass located between the track and supporting soil.

This paper presents a numerical model capable of modelling railway vibration in the presence of an embankment. The model is a 3D FEM model capable of simulating both dynamic and quasi-static excitation mechanisms. Model results are verified using experimental field data and then it is used to determine the effect different embankment conditions have on the transmission and propagation of railway vibration.

II. MODELLING APPROACH

III. TRACK MODELLING

The International union of Railways [9] and the UK channel tunnel rail link [8] specifications were used as a basis for the railway track dimensions and material properties. As the problem domain was symmetrical in the train passage direction, only half of each component was modelled. 77 sleepers were modelled and were supported by a ballast, sub-ballast and sub-grade layer respectively. The track component layout can be seen in Figure 1.

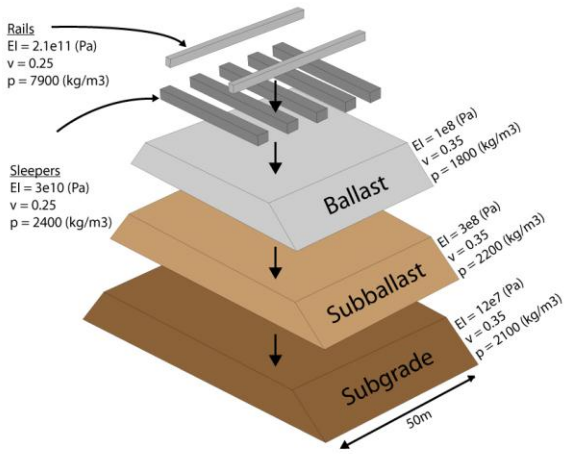

Figure 1. FEM track component layout

This work was funded by EPSRC grant Ep/H029397/1.

IV. Soil Modelling

The supporting soil was modelled as a stratified body with three layers. The bottom layer was a 3.4m sand layer which was terminated by a layer of infinite elements to simulate an infinity condition. The middle layer was a clay layer 3.9m thick and the surface layer was a 2.7m body of silt. Physically this represented a typical soil where compressional and shear wave speeds increase with depth. Material parameters are found in Table 1.

	Young's modulus (Mpa)	Poisson's ratio	Density (kg/m3)
Rail	210,000	0.25	7,900
Sleepers	30,000	0.3	2,400
Ballast	100	0.35	1,800
Subballast	300	0.35	2,200
Subgrade	127	0.35	2,100
Soil layer 1	129	0.3	1,600
Soil layer 2	227	0.3	2,000
Soil layer 3	659	0.3	2,000
Soft embankment	60	0.23	1,300
Stiff embankment	600	0.35	2,150

Table 1. Track and soil material properties

V. Absorbing Boundary Condition

To simulate an infinitely long section of soil in all three directions an absorbing boundary condition was placed on each truncated boundary (Figure 2). This prevented large spurious reflections from the boundaries contaminating the solution.

To achieve this, infinite elements were utilised. To utilise infinite elements within ABAQUS required the input file to be directly edited using several MATLAB scripts. These were required to perform tasks such as nodal renumbering and nodal projection.

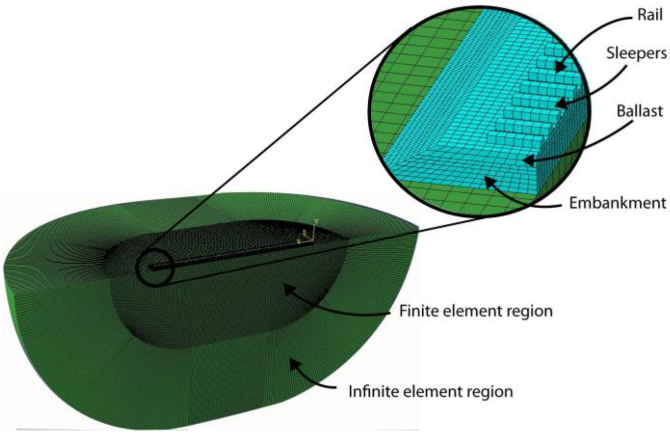

Figure 2. Finite/infinite element solution

VI. Locomotive Modelling

The locomotive was modelled at a Thalys high speed train of length 200m formed from 11 carriages. This configuration consisted of two driving cars, two traction cars and 7 passenger cars as commonly found operating in continental Europe. The first three cars (driving, traction and passenger) are illustrated in Figure 3.

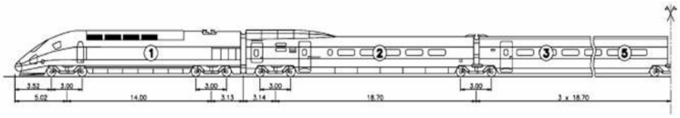

Figure 3. Thalys high speed train schematic

A non-linear Hertzian contact spring [13] was used to couple the wheel and rail components. This allowed the magnitude of the force exerted from the wheel into the rail to vary with both time and displacement, rather than just with time (e.g. constant moving load). Furthermore the non-linear contact allowed for loss of contact between the wheel and rail.

$$F_{wr} = k_H (u_w - u_r - r)^{1.5}, \quad u_w - (u_r + r) < 0$$
$$F_{wr} = 0 \qquad u_w - (u_r + r) > 0$$

F_{wr} represents the wheel/rail interaction force and K_{wr} is the Hertzian constant which is related to the geometry and material properties of the wheel and rail. A value of K_{wr}=9.4e10 was assumed. r represents the rail surface irregularity. A breakdown of the locomotive multi-body model is shown in Figure 4.

.

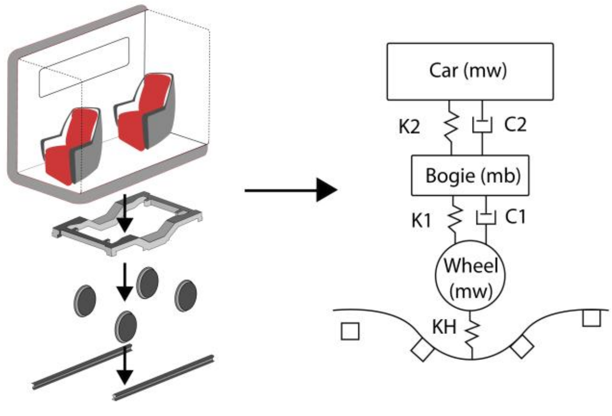

Figure 4. Vehicle FEM model breakdown

VII. Numerical Simulation

To allow the train loads to be a function of displacement, the VDLOAD subroutine typically used to define moving loads was modified. This modification allowed the real time rail displacement values to be accessed from within the VDLOAD subroutine, which was then used to calculate the magnitude of the force. Therefore two distinct integration schemes were used in a staggered manner, i.e. the first was the default ABAQUS solver used to calculate the response of the rail and all other components of the main model, and the second was used to solve the equations of motion for the vehicle based upon the previously calculated rail displacements. For the second set of equations, an explicit central difference integration scheme [14] was used:

$$\mathbf{X}_{t+1} = \mathbf{X}_t + \Delta t\mathbf{V}_t + 0.5\Delta t\mathbf{X}_t$$
$$\mathbf{A}_{t+1} = \mathbf{M}^{-1}\left(\mathbf{F}_{ext} - \mathbf{C}\mathbf{X}_t - \mathbf{K}\mathbf{X}_{t+1}\right)$$
$$\mathbf{V}_{t+1} = \mathbf{V}_t + 0.5\Delta t\left(\mathbf{A}_t + \mathbf{A}_{t+1}\right)$$

Where **X**, **A** and **V** are displacement, acceleration and velocity respectively. $\mathbf{F}_{ext}$ is the external force vector and Δt is the timestep. The integration scheme closely followed that used within the ABAQUS solver thus making it trivial to ensure that the minimum timestep threshold was met simultaneously for both staggered schemes.

VIII. Validation with Experimental Data

The final model was benchmarked by comparing simulation results to experimental results collected in Belgium in 2005[12]. For the validation tests the timestep was fixed at 1.6×10^{-5}s and the model was subject to the passage of a Thalys high speed train travelling at 265km/h.

The resulting traces for the experimental and numerical results, for a point located at 19m from the track, are shown in Figure 5.

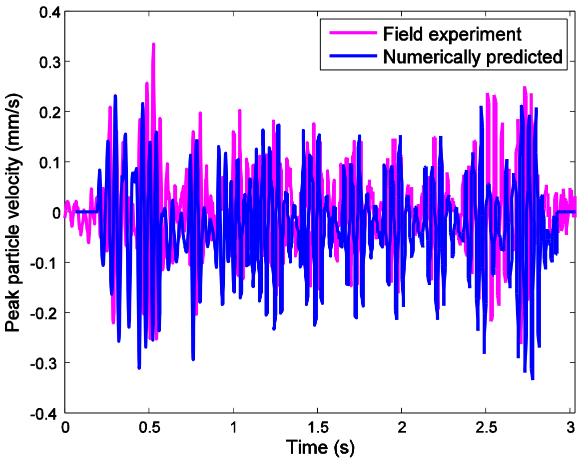

Figure 5. Experimental time history v.s. numerically predicted

The numerical and experimental vibration time histories show strong similarities between shape, timing and magnitude. Furthermore, each of the 11 wheel-sets are clearly noticeable with the heavier wheel-sets associated with the driving and traction cars visible at the start and end of the traces.

Although the numerical prediction appears to overestimate the downward velocities and underestimates the positive peak of the first traction car wheel-set, the overall correlation is high.

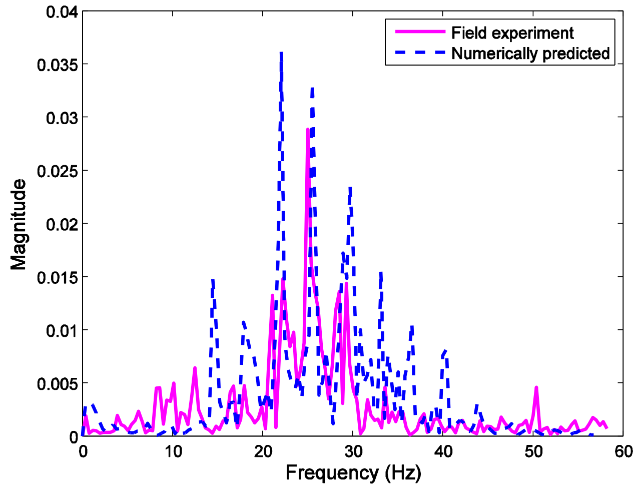

Figure 6. Experimental frequency spectrum v.s. numerically predicted

Figure 6 shows the frequency content of the two traces compared in figure 5. Again the numerical model performs well and is able to replicate the three dominant frequencies at 22, 25 and 29Hz.

After analysing the time histories and frequency content of the predicted and experimental responses it can be concluded that the numerical model has strong prediction capabilities.

IX. Numerical Results

In an attempt to investigate the effect of embankment presence on the transmission and propagation of ground vibration, three modelling cases were used. The first two of these cases were 1.5m high embankments with a slope of 30 degrees, but with different material properties. The third case was a control case and no embankment was present, instead the track section was 'at-grade'.

The two embankments were formed from two different materials. These materials were chosen to be very soft and very stiff respectively. Their purpose was to allow an insight into the effect of generalised material properties rather than to represent commonly found embankment scenarios. For each case, vibration levels in two distinct modelling domains was analysed, the near field and the far field.

X. The Effect on Near Field Vibrations

If vibration is large in the near field (i.e. locations within the track structure) there can be significant implications for passenger safety due to possible train derailment. Therefore to gauge the response of track response, the vertical deflection of a point on the ballast surface was monitored.

Figure 7 shows the passage of the first four wheels of a Thalys high speed train. Each bogie and wheel passage are clearly visible. It shows that a stiff embankment causes a reduction in vibration levels in comparison to the case of no embankment. In contrast, the case of a soft embankment gives rise to larger vibration levels in comparison to the at-grade case. If the soft and stiff cases are compared, the soft case generates displacement magnitudes 63% greater.

These changes in vibration levels are caused by two primary factors; overall embankment compressional strength and embankment/soil reflection coefficient. Firstly for the soft embankment the low compressional strength means that the loads exerted by the Thalys train penetrate to greater depth thus causing greater ballast deflection. Secondly, the change in material properties between embankment and soil is much greater for the soft embankment in comparison to the stiff embankment. The soft embankment case translates to a reflection coefficient of 0.28 whereas the stiff case translates to a reflection coefficient of -0.55. Therefore the soft embankment causes energy to become trapped within it while the stiff embankment allows a free transmission of energy into the surrounding soil.

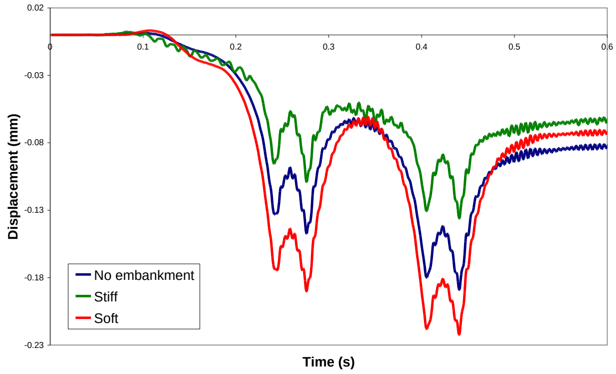

Figure 7. Ballast deflection due to Thaly's passage – a comparison of embankment conditions

XI. The Effect on Far Field Vibrations

The effect of far field vibration levels is important for structures located near high speed lines. To assess the effect of embankment conditions on the far field Peak Particle Velocities (PPV's) were analysed

The change in PPV with distance from embankment footing is shown in Figure 8. As the distance changes from 2m to 14m, PPV decreases relatively linearly for all three cases. Despite this, the case of the stiff embankment causes greater vibration at every location than the case of no embankment while the case of the stiff embankment causes lower vibration than the case of no embankment. If the soft and stiff cases are compared, there is an average vibration level decrease of 72% by changing the embankment material properties from soft to stiff.

If can be concluded that embankments constructed from stiffer material reduce vibration levels not just in the near field, but in the far field too.

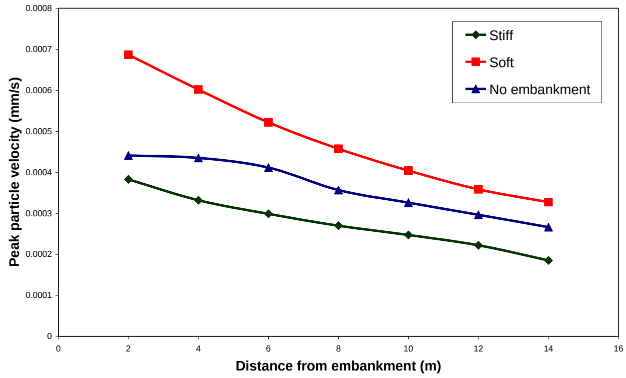

Figure 8. Far field PPV variation with distance - a comparison of embankment conditions

XII. Conclusion

A three dimensional numerical model has been created for the purpose of analysing the transmission and propagation of vibration from railway lines. The model is able to simulate both quasi static and dynamic excitation mechanisms through a non-Hertzian contact coupling between wheel and rail. The equations of motion for the locomotives are solved in a staggered manner with respect to the default solver.

The model is then used to compare the vibration levels generated in the near and far fields by three embankment cases: soft, stiff and no embankment. It is found that stiffer embankments give rise to lower levels of vibration both within the track structure and at larger distances from the track, in comparison to softer embankments.

It is concluded that this is caused by two primary factors. Firstly, if an embankment constituent material is softer than the underlying soil then energy is trapped within the embankment structure causing a waveguide effect. Secondly, a softer embankment material has less compressional strength thus allowing the train wheels to penetrate to greater depth.

Acknowledgement

The author greatly acknowledges the supervision of Prof. Mike Forde and Dr. Antonis Giannopoulos. Further acknowledgement is given to the University of Edinburgh, Prof. Peter Woodward (Heriot-Watt University) and EPSRC grant Ep/H029397/1.

References

[1] J. Kenny, Steady-state vibrations of beam on elastic foundation for moving load, *Journal of Applied Mechanics1*, vol. 76, pp. 359–364, 1954.

[2] L. Fryba, *Vibration of Solids and Structures Under Moving Loads*. Groningen, The Netherlands: Noordhoff International Publishing, 1972.

[3] V. Krylov, A. Dawson, M. Heelis, and A. Collop, Rail movement and ground waves caused by high-speed trains approaching track-soil critical velocities, *Proceedings of the Institution of Mechanical Engineers, Part F: Journal of Rail and Rapid Transit*, vol. 214, no. 2, pp. 107–116, Jan. 2000.

[4] M. Banimahd, J. Kennedy, P. Woodward, and G. Medero, Behaviour of train – track interaction in stiffness transitions, *Proceedings of the Institution of Civil Engineers*, vol. 1, no. 2006, pp. 1–10, 2010.

[5] G. Kouroussis, O. Verlinden, and C. Conti, Ground propagation of vibrations from railway vehicles using a finite/infinite-element

model of the soil, *Proceedings of the Institution of Mechanical Engineers, Part F: Journal of Rail and Rapid Transit*, vol. 223, no. 4, pp. 405–413, Jul. 2009.

[6] P. Galvin, A. Romero, and J. Domínguez, Fully three-dimensional analysis of high-speed train–track–soil-structure dynamic interaction, *Journal of Sound and Vibration*, vol. 329, no. 24, pp. 5147–5163, Nov. 2010.

[7] A. Ditzel and G. Herman, The influence of a rail embankment on the vibrations generated by moving trains, *Journal of Sound and Vibration*, vol. 271, no. 3–5, pp. 937–957, Apr. 2004.

[8] International union of Railways, UIC code 719R: Earthworks and trackbed layers for railway lines, UIC, Paris, France, 1994.

[9] N. O'Riordan and A. Phear, Design and construction of ballasted track formation and subgrade for high speed lines, in *Proceedings of the International Conference of "Railway Engineering-2001"*, Engineering Technics Press, UK, CD-Rom, ISBN 0-947644-45-8.

[10] K. Johnson, *Contact mechanics*. Cambridge, UK: Cambridge University Press, 1985.

[11] I. Smith and D. Griffiths, *Programming the finite element method*. NY: Wiley, 1997.

[12] G. Kouroussis, O. Verlinden, and C. Conti, Free field vibrations caused by high-speed lines: Measurement and time domain simulation, *Soil Dynamics and Earthquake Engineering*, vol. 31, no. 4, pp. 692–707, Apr. 2011.